

Crosstalk Insensitive Trapped-Ion Entanglement through Coupling Matrix Engineering

Vikram Kashyap,^{1,2,3} Caleb Walton,³ and Sara Mouradian³

¹Joint Center for Quantum Information and Computer Science, University of Maryland - 20742, USA

²Department of Physics, University of Maryland - 20742, USA

³Department of Electrical and Computer Engineering, University of Washington - 98195, USA

Control crosstalk due to imperfect optical addressing in trapped-ion entangling gates results in unwanted entanglement between the target ions and their neighbors. These errors are highly non-local, making them particularly difficult to correct using error correcting codes. We introduce a method to design entangling gates that are insensitive to optical crosstalk by controlling the excitation of the ions' motional modes to engineer an effective qubit-qubit coupling matrix that entirely excludes crosstalk-affected ions from the entangling operation. This method requires no knowledge of the crosstalk level and relies only on optimization of the laser pulse, avoiding the need to modify the optical setup or use additional gate operations. We experimentally demonstrate the method on a three-ion string by performing an entangling gate that is completely insensitive to optical crosstalk.

Trapped-ion systems are a leading platform for quantum information processing with operation errors below the error correction threshold in small-scale systems [1, 2]. However, imperfect optical addressing is an increasingly important source of infidelity. Optical crosstalk can, in principle, be directly minimized with careful optical engineering [3–5]. However, this is increasingly difficult for large-scale systems [6–8], especially as the field moves towards integrated optics, where optical aberrations are more prominent [9–14]. Optical crosstalk can also be directly canceled with equal-amplitude, opposite phase signals [15, 16], though this requires precise calibration. Even in a system with no optical aberrations, reducing the beam waist of the addressing beam to reduce optical crosstalk will also introduce other errors that may be more difficult to correct: polarization becomes ill-defined at a tightly focused beam waist [17, 18], and errors will arise due to relative ion-beam motion, either due to beam pointing instability [5, 11] or, more fundamentally, thermal motion of the ion [19–21].

High fidelity single-qubit gates in the presence of optical crosstalk are possible using composite pulse sequences [22] or quantum error correction [23]. However, optical crosstalk errors in entangling gates are more difficult to correct using error-correcting codes because unwanted entanglement is generated between nonlocal sets of qubits. Thus, crosstalk error mitigation methods at the gate level are necessary [23–25].

Previous proposals for crosstalk-insensitive entangling operations use mid-gate single-qubit flips on the target or neighbor ions to echo out unwanted entangling operations between target and neighbor ions [24, 26]. In this manuscript, we instead directly construct entangling gates that are insensitive to crosstalk by exciting the vibrational modes of the ion string in ratios that produce an effective ion-ion coupling matrix that excludes interactions between the target ions and their crosstalk-affected neighbors.

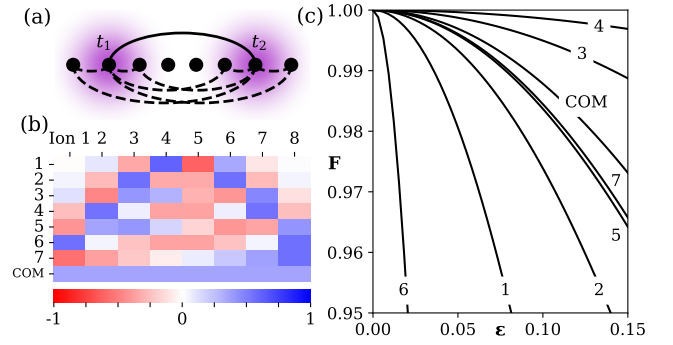


FIG. 1. (a) Optical addressing of the target ions t_1, t_2 results in crosstalk on neighboring ions, leading to target-neighbor interactions (dotted lines) in addition to the target interaction (solid line). (b) Mode participation values $b_{m,j}$ for 8 ions in a harmonic potential. (c) Fidelity reduction due to crosstalk for $\Theta = \pi/4$ entangling gates which excite only one mode, highlighting the importance of the structure of $b_{m,j}$.

We consider a 1-dimensional string of N trapped ions with internal qubit degrees of freedom and global vibrational modes. The two-qubit entangling gates we design use one set of radial modes with frequencies ν_m , Lamb-Dicke parameters η_m , and mode participation values $b_{m,j}$ for each mode m and ion j . Our aim is to entangle two target ions (t_1 and t_2) while leaving the remaining ions unaffected.

The ideal two-qubit entangling unitary is $\hat{U}_{\text{ideal}} = \exp(i\Theta \hat{X}_{t_1} \hat{X}_{t_2})$, where \hat{X}_j is the standard single-qubit gate operating on ion j , and Θ is the desired angle; $\Theta = \pi/4$ prepares a maximally entangled state. This entangling operation can be implemented with a spin-dependent force $f_j(\tau)$ applied to each ion j [27, 28] with a strength proportional to the electric field incident on ion j .

Fig. 1 shows a chain of eight ions in a harmonic trapping potential (a) and the $b_{m,j}$ values for each radial

mode (b). Ideally, the entangling lasers would be addressed to only the target ions t_1 and t_2 but some fraction of the light spills onto the four neighboring ions. This optical crosstalk leads to unwanted entangling gates between the target and neighbor ions (dotted lines in Fig. 1(a)), decreasing the fidelity of the operation.

We restrict our focus to identical pulses applied to each target ion, implying that the spin-dependent forces differ only in magnitude from ion to ion: $f_j(\tau) = \Omega_j f(\tau)$, where Ω_j is the peak Rabi frequency of light incident on ion j . The interaction Hamiltonian in the Lamb-Dicke regime is [29]

$$\hat{H}(\tau) = \sum_{j,m} \eta_m b_{m,j} \Omega_j f(\tau) \hat{X}_j \hat{a}_m^\dagger e^{i\nu_m \tau} + \text{h.c.}, \quad (1)$$

where \hat{a}_m^\dagger is the raising operator for mode m and we have set $\hbar = 1$.

The operation must not leave the ions' qubit states entangled with their motional states at the gate time τ_{gate} . This can be guaranteed by picking $f(t)$ to satisfy $\int_0^{\tau_{\text{gate}}} e^{i\nu_m \tau'} f(\tau') d\tau' = 0$ for each mode m [30]. These N complex-valued linear constraints impose $2N$ real-valued constraints that can be satisfied using parameterized pulse shapes such as segmented amplitude-modulated (AM) pulses [31] or multi-tone pulses [32]. The unitary operation implemented on the qubit states at the gate time then takes the form of pairwise coupled rotations [29, 31]

$$\hat{U}(\tau_{\text{gate}}) = \prod_{j_1 < j_2} \exp(i\theta_{j_1, j_2}(\tau_{\text{gate}}) \hat{X}_{j_1} \hat{X}_{j_2}), \quad (2)$$

of angles

$$\theta_{j_1, j_2}(\tau) = 2\Omega_i \Omega_j J_{j_1, j_2}(\tau), \quad (3)$$

where J the qubit coupling matrix. We decompose each entry of the coupling matrix as $J_{j_1, j_2}(\tau) = g^{(j_1, j_2)} \cdot \chi(\tau)$. The dependence of the coupling between ions j_1 and j_2 on their participation in each motional mode m is described by the vector $g_m^{(j_1, j_2)} = b_{m, j_1} b_{m, j_2}$. The dependence of $J_{j_1, j_2}(\tau)$ on $f(\tau)$ is described by

$$\chi_m(\tau) = \eta_m \int_0^\tau \int_0^{\tau'} \sin(\omega_m(\tau' - \tau'')) f(\tau') f(\tau'') d\tau'' d\tau', \quad (4)$$

which is proportional to the spin-dependent phase angle accrued in each mode m .

With perfect optical control we could set $\Omega_j = 0$ for all non-target ions to ensure that $\theta_{j_1, j_2} = 0$ for all pairs of ions other than the target pair. However, due to spillover of the controlling laser, each neighbor ion will receive some fraction of the Rabi frequency Ω_t applied to each target ion t in the set $\mathcal{T} := \{t_1, t_2\}$. Although this fraction may be different for each neighbor ion depending on its physical position, we can characterize the crosstalk by

a maximal fraction ϵ such that $\Omega_n < \epsilon \Omega_t$ for all $n \in \mathcal{N}$, the set of neighbor ions. As per Eq. 2, the nonzero Ω_n leads to a target-neighbor crosstalk error described by a unitary that acts in addition to the target gate \hat{U}_{ideal} and is given by

$$\hat{U}_{\text{crosstalk}} = \sum_{t \in \mathcal{T}} \sum_{n \in \mathcal{N}} \exp\left(i \frac{\Omega_n}{\Omega_t} \frac{J_{t,n}}{J_{t_1, t_2}} \Theta \hat{X}_t \hat{X}_n\right). \quad (5)$$

The angle of a crosstalk rotation depends on the relative strengths of the couplings of the target and crosstalk pairs. If the coupling between the target ions is less than the coupling between a target and neighbor ion by a ratio on the order of the crosstalk fraction (i.e. $|J_{t_1, t_2}|/J_{t,n} \lesssim \epsilon$), then the crosstalk rotation angle $\theta_{t,n}$ will be on the order of the target gate angle Θ and so lead to a large drop in target gate fidelity.

This is of significant concern in long ion chains. The coupling between two ions separated by a distance r has a bound scaling as $1/r^3$ [29, 33], meaning that it is particularly likely that $|J_{t,n}| > |J_{t_1, t_2}|$ for direct target-neighbor pairs ($n = t \pm 1$). Thus, on short time scales with respect to the length of the string the coupling between the target ions has a much smaller bound than the bound on the coupling between each target ion and its two neighbors.

Even in a short chains, crosstalk errors can be large due to the structure of $b_{m,j}$. This is illustrated in Fig. 1(c) where we consider a slow Mølmer-Sørensen gate which generates phase in only one motional mode – $\chi_m = 0$ for all $m \neq m'$, such that $J_{j_1, j_2} = b_{m', j_1} b_{m', j_2}$. If $b_{m', t} \leq b_{m', n}$ for the target-neighbor pairs, mode m' will be especially susceptible to crosstalk errors, as is the case for mode 6 when entangling qubits 2 and 7 in the 8-ion string.

In this manuscript we exploit this structure to construct gates that are inherently insensitive to crosstalk. To do this, we must create a qubit coupling matrix where $J_{t,n} = 0$ for $t, n \in \mathcal{T} \times \mathcal{N}$ and J_{t_1, t_2} is as large as possible. Designing a qubit coupling graph J through the preferential excitation of vibrational modes has been considered in the context of analog quantum simulation of spin models with global addressing [32, 34]. Since there are only N degrees of freedom in χ and $(N^2 - N)/2$ parameters in J , it is impossible to produce arbitrary inter-qubit couplings in this manner. However, we show that creating crosstalk-insensitive coupling matrices is possible for most target ion pairs when considering experimentally realizable motional mode structures.

For a given set of targets, we must find a vector of spin-dependent phases χ^{in} such that $J_{j_1, j_2} = g^{(j_1, j_2)} \cdot \chi^{\text{in}}$ eliminates each of the ≤ 8 target-neighbor crosstalk interactions while still allowing the desired target-target interaction to be run within a given power budget. For a pair of target ions (t_1, t_2) , we define the set of target-neighbor crosstalk mode-dependence vectors $\mathcal{R}^{(t_1, t_2)} = \{g^{(t,n)} | t, n \in \mathcal{T} \times \mathcal{N}\}$. The space of spin-dependent phase vectors from which we can pick χ^{in} is then the $\geq (N - 8)$

dimensional $\text{Null}(R^{(t_1, t_2)})$, the null space of the matrix $R^{(t_1, t_2)}$ which has the vectors in $\mathcal{R}^{(t_1, t_2)}$ as columns. This crosstalk-insensitive space always exists for $N \geq 9$, and solutions often exist for shorter strings, as evidenced in Fig. 2. To achieve the desired target-target interaction while eliminating all target-neighbor interactions, $g^{(t_1, t_2)}$ must have a component in $\text{Null}(R^{(t_1, t_2)})$ and this component must be sufficiently large such that achieving the desired angle Θ does not require an experimentally infeasible power or time (Eq. 3).

Whether or not an efficient crosstalk-insensitive χ^{in} exists depends on the set of motional modes available and the particular pair of target ions being considered. Evenly spaced ion strings, which have advantages in string stability, cooling, optical control, and measurement [35, 36], have sinusoidal modes that can be used to produce a variety of inter-qubit couplings for quantum simulation [34]. The structure of these modes allows for crosstalk-insensitive gates to be run on all pairs of ions that do not include the two outermost ions. In the Supplemental Materials Section S1 we provide a proof that any such target gate described by $g^{(t_1, t_2)}$ has a large component that is linearly independent of all crosstalk interactions in $\mathcal{R}^{(t_1, t_2)}$ [37]. While there are no analytic expressions for the motional modes of ions in harmonic trapping potentials, we numerically find that target pairs of ions that are either nearest-neighbors or symmetric to each other across the center of the string (i.e. pairs of the form $(j, N + 1 - j)$) have target interaction mode-dependence vectors that are sufficiently independent of the crosstalk interaction vectors to allow for crosstalk-insensitive gates.

Armed with a set of possible χ^{in} solutions, we must now find an appropriate $f(\tau)$ that implements a $\chi(\tau_{\text{gate}})$ (Eq. 4) that is within the space spanned by those phase vectors. The primary difficulty in calculating an appropriate $f(\tau)$ lies in the quadratic dependence of $\chi(\tau)$ on $f(\tau)$ (Eq. 4). However we point out that the dependence can be made effectively linear by dividing the total gate time into L “loops” of duration τ_{loop} during each of which we apply a pulse with shape $f^{(l)}(\tau)$ that causes each mode to trace out a closed loop in phase space. Since the qubits are disentangled from the modes at the end of each component pulse, each loop independently generates spin-dependent phases in the motional modes according to a vector $\chi^{(l)}$. At the gate time $\tau_{\text{gate}} = L \times \tau_{\text{loop}}$, the total spin-dependent phase vector is $\chi(\tau_{\text{gate}}) = \sum_l \chi^{(l)}$, which depends linearly on the amplitude scaling of each component pulse $f^{(l)}(\tau)$. The periodically-closed phase space paths and the linear combinations of inter-qubit couplings they produce are illustrated with an example in Fig. 2. As long as the $\chi^{(l)}$ vectors span a space of dimension ≥ 9 , we can always produce a net $\chi(\tau_{\text{gate}})$ that lies in the $N - 8$ dimensional space $\text{Null}(R^{(t_1, t_2)})$. However, even in shorts strings a smaller number of loops can be used in cases with high symmetry. The phase space paths

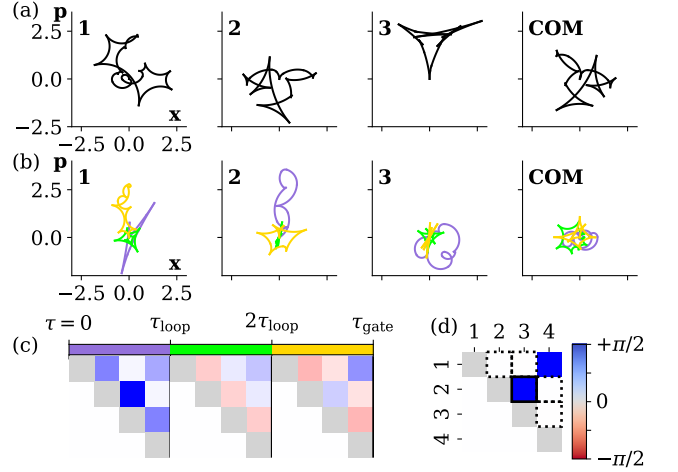


FIG. 2. (a) Phase space paths of each mode for a pulse shape directly optimized to solve the quadratic expression Eq. 7. (b) Phase space paths for each mode and loop of a linearized pulse. (c) Coupling matrices produced by each loop of the linearized pulse. (d) Crosstalk-insensitive coupling matrix created both by the quadratically optimized pulse solution in (a) and the linearized pulse solution in (b). The coupling values plotted here are $\hat{X}\hat{X}$ rotation angles for a global laser drive. In the case of optical crosstalk from individually addressed target ions, the neighbor-neighbor (1,4) rotation angle would be suppressed quadratically in the crosstalk fraction ϵ , leaving the (2,3) rotation as the only significant interaction.

in Fig. 2(b) result from only $L = 3$ composite pulses each consisting of 10 AM segments over $\tau_{\text{loop}} = 55\mu\text{s}$, where the l th set of 10 segments uses a bichromatic laser with detunings -1 kHz from the l th sideband. There is no guarantee that the the phase vectors $\chi^{(l)}$ will span the necessary dimension in all situations – in particular for $\tau_{\text{gate}} \ll 2\pi/\nu_m$ for all m , $\chi(\tau_{\text{gate}})$ will become independent of $f(\tau)$ as per Eq. 4 – but for common gate durations our numerical results indicate that this linearized method can be used to produce crosstalk-insensitive entangling pulses with easily-attainable peak powers. In Section S2 of the Supplemental Material we demonstrate the method by calculating linearized crosstalk-insensitive entangling pulses for gates on all neighboring and symmetric pairs of target ions in a harmonically trapped 12-ion string [37].

To validate our gate construction method, we use the QSCOUT platform [16, 37] to run entangling gates on the outer two ions of a three-ion chain while increasing the optical field on the center ion to artificially simulate crosstalk. The inset of Fig. 3(a) shows the mode coupling matrices $J_{j_1, j_2}^{(m)} = b_{m, j_1} b_{m, j_2}$ for each of the modes in a three-ion chain. As expected from the mirror symmetry of the chain, the “tilt” mode (mode 2) provides natural crosstalk immunity since $g_2^{1,2} = g_2^{2,3} = 0$. In contrast, the center ion has strong participation in the other two modes. To illustrate this, we run three Mølmer-Sørensen-type entangling operations with $\Theta = \pi/4$, each targeting

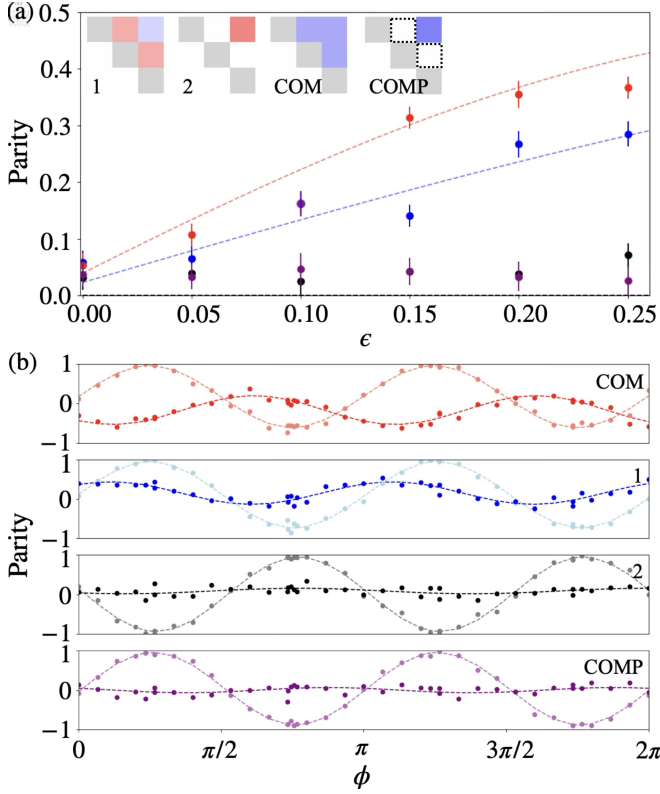


FIG. 3. a) Parity between the target and center ion for single mode excitation (black, blue, and red) and composite gate (purple) as a function of crosstalk. The inset shows the $J^{(m)}$ matrices for the three modes and composite gate. b) The parity between the two target ions (pale) and target-center ions (dark) for each gate at $\epsilon = 0.25$.

a single mode. The gates are run with a duration of $250 \mu\text{s}$, and a -15 kHz detuning from the target radial mode. Fig. 3(a) shows entanglement fidelity through the parity between the center and target ions after applying single-qubit rotations $Z(\phi)$ to each ion to measure entanglement [28, 38]. As expected, no entanglement is generated between the target and center ion when only mode 2 is excited (black). However, when using mode 1 (blue) and the COM mode (red) to mediate entanglement generation, the parity increases significantly, matching theoretical expectations (dotted line). Figs. 3(b-d) show the full parity curves for both target-neighbor and target-target pairs at $\epsilon = 0.25$ verifying that the increase in target-neighbor entanglement is reflected in a decrease in target-target fidelity.

Utilizing only the tilt mode corresponds to the crosstalk-insensitive spin-dependent phase vector $\chi^{\text{in}} \propto (0, 1, 0)$, but using our framework we note that the crosstalk-insensitive space for this gate also includes $\chi^{\text{in}} \propto (1, 0, 1)$. We demonstrate our linearized pulse solution method by constructing a solution with two loops that produce this multi-mode χ^{in} : a $\theta_{t_1, t_2} = \pi/6$ pulse is run targeting mode 3 (COM) followed by a $\theta_{t_1, t_2} = \pi/12$

pulse on mode 1, both with the same parameters as described above. The purple data points in Fig. 3(a,b) demonstrate that this method also produces a crosstalk-insensitive gate even though each individual loop generates temporary entanglement between the center and target ions.

If we relax the stipulation that the qubits are disentangled from the modes at every multiple of τ_{loop} , it is possible – though more computationally intensive – to find a better power- or time-efficient pulse by searching the full space of pulses that only disentangle from the modes by time τ_{gate} . This is a problem that has already been investigated in Ref. [32], where multi-tone pulses are optimized over the amplitudes of each tone to generate desired spin-dependent phases in each vibrational mode. We outline a method for performing the same task using experimentally simpler AM pulses.

Consider a bichromatic laser with tones symmetrically detuned by ω_d from the qubit transition to near the vibrational sideband frequencies. The time dependence of the Rabi frequency is split into D equal segments such that $\Omega(\tau) = w_{\lfloor D\tau/\tau_{\text{gate}} \rfloor}$, where w is a vector of $D = 2N + D'$ Rabi frequency amplitudes. The associated spin-dependent force has the form $f(\tau) = \Omega(\tau) \sin(\omega_d \tau)$. Due to the linear mode-closure constraints on $f(\tau)$, there is a space of $D' := (D - 2N)$ amplitude vectors that close the modes' phase space paths by the end of the gate. Thus any mode-closing pulse shape can be expressed as $w = Kx$, where K is a matrix with columns spanning space of mode-closing amplitude vectors. Because of the quadratic dependence of $\chi(\tau_{\text{gate}})$ on $f(\tau)$, we can express it as

$$\chi_m(\tau_{\text{gate}}) = \tilde{\chi}_m(x) := w^T P^{(m)} w = x^T K^T P^{(m)} K x \quad (6)$$

where $P^{(m)}$ is a matrix that splits the double time integral of $f(\tau)$ in Eq. 4 into $D \times D$ blocks [37].

To find a crosstalk-insensitive gate, we must optimize x to minimize the projection of $\chi(\tau_{\text{gate}})$ onto the crosstalk interaction mode-dependence vectors:

$$x_{\text{in}} = \text{argmin}_x (\|R^{(t_1, t_2)} \tilde{\chi}(x)\|_1). \quad (7)$$

Optimizing Eq. 7 is a quadratic optimization problem and the computational complexity is NP-hard in D' [32], but this does not pose an issue for short strings where few degrees of freedom are necessary and D' can be small. In Fig. 2(a) we display the phase-space paths of each mode evolving under an AM pulse optimized to implement a crosstalk-insensitive gate (Fig. 2(d)) on the center ions (ions 2 and 3) of a string of four $^{171}\text{Yb}^+$ ions. The resulting interaction matrix is identical to that produced by the linearized pulse solution (Figs. 2(b,c)) [37].

We have presented a method to design crosstalk-insensitive entangling gates, eliminating a significant source of coherent error in trapped-ion devices. Other sources of coherent error, such as coupling to the qubit

transition (carrier coupling) can likewise be eliminated using similar pulse engineering techniques with no need for changes in the optical setup or additional gates [32]. Further work on engineering inter-qubit couplings could be directed to address neighbor-neighbor crosstalk, which is second order in ϵ but may be under-recognized because it does not affect the fidelity of the target gate and may still be significant in longer and tightly-spaced strings. Another promising avenue for leveraging the techniques we have described here is to implement sets of vibrational modes [39–41] specially designed to be compatible with crosstalk-insensitive qubit couplings.

ACKNOWLEDGMENTS

We thank Kristi Beck and Brant Bowers for insightful discussions, and Ashlyn Burch and Melissa Revelle for discussions and help with implementing the experiments on QSCOUT. This material was funded in part by the U.S. Department of Energy, Office of Science, Office of Advanced Scientific Computing Research Quantum Testbed Program. This work was funded in part by the AFOSR Young Investigator Program, FA9550-24-1-0146 and NSF grant OMA-2329020. V.K. is supported by the QuICS Lanczos Graduate Fellowship. C.W. is supported through the Advancing Quantum-Enabled Technologies (AQET) traineeship program at the University of Washington.

-
- [1] M. C. Smith, A. D. Leu, K. Miyaniishi, M. F. Gely, and D. M. Lucas. Single-qubit gates with errors at the 10^{-7} level. *Phys. Rev. Lett.*, 134:230601, Jun 2025.
 - [2] C. M. Löschnauer, J. Mosca Toba, A. C. Hughes, S. A. King, M. A. Weber, R. Srinivas, R. Matt, R. Nourshargh, D. T. C. Allcock, C. J. Ballance, C. Matthiesen, M. Malinowski, and T. P. Harty. Scalable, high-fidelity all-electronic control of trapped-ion qubits, 2024.
 - [3] Rui-Rui Li, Yi-Long Chen, Ran He, Shu-Qian Chen, Wen-Hao Qi, Jin-Ming Cui, Yun-Feng Huang, Chuan-Feng Li, and Guang-Can Guo. A low-crosstalk double-side addressing system using acousto-optic deflectors for atomic ion qubits. *arXiv*, 2023.
 - [4] C. Shen, Z.-X. Gong, and L.-M. Duan. Individual addressing in quantum computation through spatial refocusing. *Phys. Rev. A*, 88:052325, Nov 2013.
 - [5] Yi-Long Chen, Rui-Rui Li, Ran He, Shu-Qian Chen, Wen-Hao Qi, Jin-Ming Cui, Yun-Feng Huang, Chuan-Feng Li, and Guang-Can Guo. Low-crosstalk optical addressing system for atomic qubits based on multiple objectives and acousto-optic deflectors. *Phys. Rev. Appl.*, 22:054003, Nov 2024.
 - [6] D. Nigg, M. Müller, E. A. Martinez, P. Schindler, M. Hennrich, T. Monz, M. A. Martin-Delgado, and R. Blatt. Quantum computations on a topologically encoded qubit. *Science*, 345(6194):302–305, June 2014.
 - [7] Tom Manovitz, Yotam Shapira, Lior Gazit, Nitzan Akerman, and Roei Ozeri. Trapped-Ion Quantum Computer with Robust Entangling Gates and Quantum Coherent Feedback. *PRX Quantum*, 3(1):010347, March 2022.
 - [8] I. Pogorelov, T. Feldker, Ch. D. Marciniak, L. Postler, G. Jacob, O. Krieglsteiner, V. Podlesnic, M. Meth, V. Negnevitsky, M. Stadler, B. Höfer, C. Wächter, K. Lakhmanskiy, R. Blatt, P. Schindler, and T. Monz. Compact Ion-Trap Quantum Computing Demonstrator. *PRX Quantum*, 2(2):020343, June 2021.
 - [9] Karan K. Mehta, Colin D. Bruzewicz, Robert McConnell, Rajeev J. Ram, Jeremy M. Sage, and John Chiaverini. Integrated optical addressing of an ion qubit. *Nat. Nanotechnol.*, 11:1066–1070, December 2016.
 - [10] Karan K. Mehta, Chi Zhang, Maciej Malinowski, Thanh-Long Nguyen, Martin Stadler, and Jonathan P. Home. Integrated optical multi-ion quantum logic. *Nature*, 586:533–537, October 2020.
 - [11] R. J. Niffenegger, J. Stuart, C. Sorace-Agaskar, D. Kharras, S. Bramhavar, C. D. Bruzewicz, W. Loh, R. T. Maxson, R. McConnell, D. Reens, G. N. West, J. M. Sage, and J. Chiaverini. Integrated multi-wavelength control of an ion qubit. *Nature*, 586:538–542, October 2020.
 - [12] Mizuki Shirao, Daniel Klawson, Sara Mouradian, and Ming C. Wu. High efficiency focusing double-etched SiN grating coupler for trapped ion qubit manipulation. *Jpn. J. Appl. Phys.*, 61(SK):SK1002, June 2022.
 - [13] Ali Binai-Motlagh, Matthew L. Day, Nikolay Videnov, Noah Greenberg, Crystal Senko, and Rajibul Islam. A guided light system for agile individual addressing of Ba⁺ qubits with 10⁻⁴ level intensity crosstalk. *Quantum Sci. Technol.*, 8(4):045012, July 2023.
 - [14] Ana S. Sotirova, Bangshan Sun, Jamie D. Leppard, Andong Wang, Mohan Wang, Andres Vazquez-Brennan, David P. Nadlinger, Simon Moser, Alexander Jesacher, Chao He, Fabian Pokorny, Martin J. Booth, and Christopher J. Ballance. Low cross-talk optical addressing of trapped-ion qubits using a novel integrated photonic chip. *Light: Science & Applications*, 13(1):199, Aug 2024.
 - [15] Jeremy Flannery, Roland Matt, Luca I. Huber, Kaizhao Wang, Christopher Axline, Robin Oswald, and Jonathan P Home. Physical coherent cancellation of optical addressing crosstalk in a trapped-ion experiment. *Quantum Science and Technology*, 10(1):015012, 2024.
 - [16] Susan M. Clark, Daniel Lobser, Melissa C. Revelle, Christopher G. Yale, David Bossert, Ashlyn D. Burch, Matthew N. Chow, Craig W. Hogle, Megan Ivory, Jessica Pehr, Bradley Salzbrenner, Daniel Stick, William Sweatt, Joshua M. Wilson, Edward Winrow, and Peter Maunz. Engineering the quantum scientific computing open user testbed. *IEEE Transactions on Quantum Engineering*, 2:1–32, 2021.
 - [17] Carl G. Chen, Paul T. Konkola, Juan Ferrera, Ralf K. Heilmann, and Mark L. Schattenburg. Analyses of vector Gaussian beam propagation and the validity of paraxial and spherical approximations. *J. Opt. Soc. Am. A, JOSAA*, 19(2):404–412, February 2002.
 - [18] A. Maltsev and T. Ditmire. Above Threshold Ionization in Tightly Focused, Strongly Relativistic Laser Fields. *Phys. Rev. Lett.*, 90(5):053002, February 2003.
 - [19] Ming Li, Kenneth Wright, Neal C. Pisenti, Kristin M. Beck, Jason H. V. Nguyen, and Yunseong Nam. Generalized Hamiltonian to describe imperfections in ion-light interaction. *Phys. Rev. A*, 102(6):062616, December 2020.

- [20] Adam D. West, Randall Putnam, Wesley C. Campbell, and Paul Hamilton. Tunable transverse spin–motion coupling for quantum information processing. *Quantum Sci. Technol.*, 6(2):024003, January 2021.
- [21] M. Cetina, L. N. Egan, C. Noel, M. L. Goldman, D. Biswas, A. R. Risinger, D. Zhu, and C. Monroe. Control of Transverse Motion for Quantum Gates on Individually Addressed Atomic Qubits. *PRX Quantum*, 3(1):010334, March 2022.
- [22] J. True Merrill, S. Charles Doret, Grahame Vittorini, J. P. Addison, and Kenneth R. Brown. Transformed composite sequences for improved qubit addressing. *Phys. Rev. A*, 90:040301, Oct 2014.
- [23] Sascha Heußen, Lukas Postler, Manuel Rispler, Ivan Pogorelov, Christian D. Marciniak, Thomas Monz, Philipp Schindler, and Markus Müller. Strategies for a practical advantage of fault-tolerant circuit design in noisy trapped-ion quantum computers. *Physical Review A*, 107(4), April 2023.
- [24] Pedro Parrado-Rodríguez, Ciarán Ryan-Anderson, Alejandro Bermudez, and Markus Müller. Crosstalk suppression for fault-tolerant quantum error correction with trapped ions. *Quantum*, 5:487, June 2021.
- [25] Dripto M Debroy, Muyuan Li, Shilin Huang, and Kenneth R Brown. Logical performance of 9 qubit compass codes in ion traps with crosstalk errors. *Quantum Science and Technology*, 5(3):034002, 2020.
- [26] Chao Fang, Ye Wang, Shilin Huang, Kenneth R. Brown, and Jungsang Kim. Crosstalk suppression in individually addressed two-qubit gates in a trapped-ion quantum computer. *Phys. Rev. Lett.*, 129:240504, Dec 2022.
- [27] Anders Sørensen and Klaus Mølmer. Entanglement and quantum computation with ions in thermal motion. *Phys. Rev. A*, 62:022311, Jul 2000.
- [28] P. C. Haljan, P. J. Lee, K-A. Brickman, M. Acton, L. Deslauriers, and C. Monroe. Entanglement of trapped-ion clock states. *Physical Review A*, 72(6):062316, December 2005.
- [29] K. A. Landsman, Y. Wu, P. H. Leung, D. Zhu, N. M. Linke, K. R. Brown, L. Duan, and C. Monroe. Two-qubit entangling gates within arbitrarily long chains of trapped ions. *Phys. Rev. A*, 100:022332, Aug 2019.
- [30] J. J. García-Ripoll, P. Zoller, and J. I. Cirac. Coherent control of trapped ions using off-resonant lasers. *Phys. Rev. A*, 71:062309, Jun 2005.
- [31] T. Choi, S. Debnath, T. A. Manning, C. Figgatt, Z.-X. Gong, L.-M. Duan, and C. Monroe. Optimal quantum control of multimode couplings between trapped ion qubits for scalable entanglement. *Phys. Rev. Lett.*, 112:190502, May 2014.
- [32] Yotam Shapira, Ravid Shaniv, Tom Manovitz, Nitzan Akerman, Lee Peleg, Lior Gazit, Roei Ozeri, and Ady Stern. Theory of robust multiqubit nonadiabatic gates for trapped ions. *Phys. Rev. A*, 101:032330, Mar 2020.
- [33] J. Jünemann, A. Cadarso, D. Pérez-García, A. Bermudez, and J. J. García-Ripoll. Lieb-robinson bounds for spin-boson lattice models and trapped ions. *Phys. Rev. Lett.*, 111:230404, Dec 2013.
- [34] Antonis Kyprianidis, A J Rasmusson, and Philip Richerme. Interaction graph engineering in trapped-ion quantum simulators with global drives. *New Journal of Physics*, 26(2):023033, February 2024.
- [35] G.-D. Lin, S.-L. Zhu, R. Islam, K. Kim, M.-S. Chang, S. Korenblit, C. Monroe, and L.-M. Duan. Large-scale quantum computation in an anharmonic linear ion trap. *Europhysics Letters*, 86(6):60004, jul 2009.
- [36] Michael Johannng. Isospaced linear ion strings. *Applied Physics B*, 122:1–17, 2016.
- [37] See supplementary information.
- [38] Cass A Sackett, David Kielpinski, Brian E King, Christopher Langer, Volker Meyer, Christopher J Myatt, Mary Rowe, Quentin A Turchette, Wayne M Itano, David J Wineland, et al. Experimental entanglement of four particles. *Nature*, 404(6775):256–259, 2000.
- [39] Yi Hong Teoh, Manas Sajjan, Zewen Sun, Fereshteh Rajabi, and Rajibul Islam. Manipulating phonons of a trapped-ion system using optical tweezers. *Phys. Rev. A*, 104:022420, Aug 2021.
- [40] Tobias Olsacher, Lukas Postler, Philipp Schindler, Thomas Monz, Peter Zoller, and Lukas M. Sieberer. Scalable and parallel tweezer gates for quantum computing with long ion strings. *PRX Quantum*, 1:020316, Dec 2020.
- [41] Ming Li, Nhung H. Nguyen, Alaina M. Green, Jason Amini, Norbert M. Linke, and Yunseong Nam. Realizing two-qubit gates through mode engineering on a trapped-ion quantum computer. *Phys. Rev. A*, 111:022622, Feb 2025.
- [42] D.F.V. James. Quantum dynamics of cold trapped ions with application to quantum computation. *Applied Physics B: Lasers and Optics*, 66:181–190, February 1998.
- [43] Christopher G. Yale, Ashlyn D. Burch, Matthew N. H. Chow, Brandon P. Ruzic, Daniel S. Lobser, Brian K. McFarland, Melissa C. Revelle, and Susan M. Clark. Realization and calibration of continuously parameterized two-qubit gates on a trapped-ion quantum processor, 2025.

Supplemental Material

SI 1

Close approximations of equispaced ion strings can be produced using trapping potentials with only harmonic and quartic components and can be realized with simple electrode configurations [35]. The motional modes associated with strings of equispaced ions are closely approximated by sinusoids [34, 36]:

$$b_{m,j}^{\sin} = \sqrt{\frac{2 - \delta_{m,1}}{N}} \cos\left(\frac{(2j-1)(m-1)\pi}{2N}\right). \quad (8)$$

These vibrational modes are more suitable for the implementation of a variety of inter-ion couplings compared to the set of modes produced in harmonic trapping potentials [34]. It has already been proven in Ref. [34] that such a collection of modes can be excited using only a global drive to produce an inter-qubit coupling that acts solely between every pair of target ions that are symmetric to each other across the center of the string, i.e. pairs of the form $(j, N+1-j)$. This coupling is in fact an instance of a crosstalk-insensitive qubit coupling because there is no coupling between any symmetric pair of target ions and their non-target neighbors. We extend this result further by proving crosstalk-insensitive couplings are possible using this set of modes for every pair of target ions that does not include the outer ions of the string.

Describing these normal modes as N -element vectors defined by $b_j^{(m)} = b_{m,j}^{\sin}$, the vectors obey the orthonormality condition $b^{(m_1)} \cdot b^{(m_2)} = \delta_{m_1, m_2}$ as expected. We can also consider the set of N -element vectors similarly defined but indexed by m rather than j : $\tilde{b}_m^{(j)} = b_{m,j}^{\sin}$. Extending the range of j to be $\{1-N, 1-N+1, \dots, 2N\}$, we note that the vectors obey the orthonormality relation $\tilde{b}^{(j_1)} \cdot \tilde{b}^{(j_2)} = \delta_{j_1, j_2} + \delta_{1-j_1, j_2} + \delta_{2N+1-j_1, j_2}$. This allows us to define the motional dependence vector of the coupling between some ions j_1 and j_2 by

$$g_m^{(j_1, j_2)} = \tilde{b}_m^{(j_1)} \tilde{b}_m^{(j_2)}. \quad (9)$$

Given target ions \mathcal{T} and the set of up to four nearest neighbors \mathcal{N} , we aim to show that $g^{(t_1, t_2)}$ is linearly independent of the set of vectors $\mathcal{R}^{(t_1, t_2)} = \{g^{(t, n)} : t, n \in \mathcal{T} \times \mathcal{N}\}$. To show this linear independence it suffices to identify a vector that is perpendicular to all vectors in $\mathcal{R}^{(t_1, t_2)}$ but has nonzero projection onto $g^{(t_1, t_2)}$. We seek such a vector with the form $C_m^{(h)} = 2 \cos(h(m-1)\pi/N)$ with $h \in \{1, 2, \dots, N\}$. To deduce the appropriate value for h , we begin by recognizing that, for $j_1 < j_2 \in \{1, 2, \dots, N\}$,

$$C_m^{(h)} g_m^{(j_1, j_2)} = g_m^{(j_1+h, j_2)} + g_m^{(j_1-h, j_2)}. \quad (10)$$

Noting that $\sum_m g_m^{(j_1, j_2)} = \tilde{b}^{(j_1)} \cdot \tilde{b}^{(j_2)}$, we conclude that

$$C^{(h)} \cdot g^{(j_1, j_2)} = \delta_{h, j_2-j_1} + \delta_{h, j_1+j_2-1} + \delta_{h, 2N+1-j_1-j_2}. \quad (11)$$

If we pick $h = t_2 - t_1$ then $C^{(t_2-t_1)} \cdot g^{(t_1, t_2)} \neq 0$. To see that $C^{(t_2-t_1)}$ is orthogonal to all vectors in $\mathcal{R}^{(t_1, t_2)}$, we consider all possibilities: $t_2 - t_1 \neq t_2 - t_1 \pm 1$ for any t_1 and t_2 , $t_2 - t_1 = t_1 + t_2 - 1 \pm 1$ only for $t_1 = 1$, and $t_2 - t_1 = 2N - t_1 - t_2 \pm 1$ only for $t_2 = N$. Thus, as long as $t_1 \neq 1$ and $t_2 \neq N$, $C^{(t_2-t_1)}$ is perpendicular to all vectors in $\mathcal{R}^{(t_1, t_2)}$ but not perpendicular to $g^{(t_1, t_2)}$. We conclude that $g^{(t_1, t_2)}$ is linearly independent of $\mathcal{R}^{(t_1, t_2)}$ for any $t_1, t_2 \in \{2, 3, \dots, N-1\}$. Choosing $\chi \propto C^{(t_2-t_1)}$ would constitute a crosstalk-insensitive vector of spin-dependent motional mode phases. These results are verified numerically for a 12-ion string in Fig. 4.

SI 2

We design AM segmented pulses to implement crosstalk-insensitive entangling operations on pairs of ions in a harmonically trapped string. The vibrational modes of ion strings in harmonic axial trapping potentials take on a standard form [42]. In order to first determine which target gates can be made crosstalk insensitive, we evaluate whether an efficient spin-dependent phase vector $\chi^{(\text{in})}$ exists that drives the target interaction but not the associated crosstalk interactions. As explained in the main text, $\chi^{(\text{in})}$ only exists if the dependence $g^{(t_1, t_2)}$ of the coupling on the spin-dependence phases generated in each mode has a large projection onto the space orthogonal to the crosstalk mode dependence vectors in $\mathcal{R}^{(t_1, t_2)}$, i.e. the space $\text{Null}(\mathcal{R}^{(t_1, t_2)})$. In Fig. 4 we plot the magnitude of the projection of $g^{(t_1, t_2)}$ onto $\text{Null}(\mathcal{R}^{(t_1, t_2)})$ for every possible target pair of ions in a 12-ion string for both the vibrational modes of a harmonically trapped string and the ideal sinusoidal modes of an equispaced string (Eq. 8). While for the equispaced string, crosstalk insensitive gates are possible for almost all target ion pairs, for harmonically trapped strings the structure of the motional modes only allows for crosstalk insensitive gates between target pairs of the form $t_2 = t_1 + 1$ (neighboring targets) and $t_2 = N + 1 - t_1$ (symmetric targets).

We produce pulses to implement crosstalk insensitive entangling gates for these neighboring and symmetric target pairs in harmonically trapped strings. To produce realistic estimations of the required laser powers and pulse durations, we consider a concrete example of $^{171}\text{Yb}^+$ ions in a trap with axial trapping frequency $2\pi \times 0.5\text{MHz}$ and radial trapping frequency $2\pi \times 3\text{MHz}$, qualitatively similar to the QSCOUT platform [16]. The controlling laser uses 355nm Raman beams to apply two tones with frequencies $\omega_q \pm \omega_d(\tau)$ where ω_q is the qubit transition frequency and $\omega_d(\tau)$ is a detuning near the motional mode frequency band that is modulated over the course of the pulse.

To produce the crosstalk-insensitive laser pulses for Fig. 2, we consider a string of 4 ions, leading to a minimum inter-ion spacing of $4\mu\text{m}$. The quadratic-

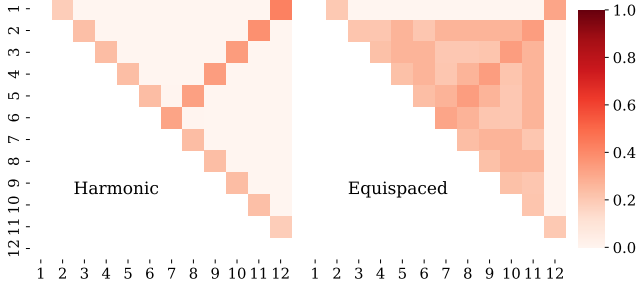


FIG. 4. Independence of the coupling of every possible pair of target ions in a 12-ion string from the associated target-neighbor crosstalk couplings, for both the vibrational modes of a harmonically trapped string and the ideal sinusoidal modes of an equispaced string (Eq. 8). A higher degree of independence indicates that the target interaction can be driven without driving the crosstalk interactions even in the presence of optical crosstalk.

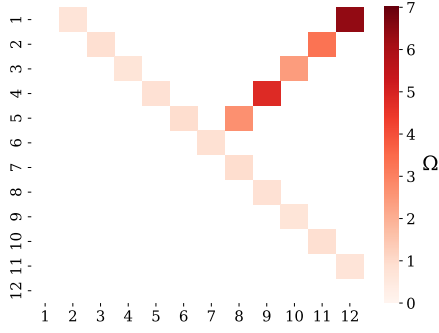


FIG. 5. Peak Rabi frequencies, in units of $2\pi \times \text{MHz}$, for $500\mu\text{s}$ AM segmented pulses implementing crosstalk-insensitive entangling gates between neighboring and symmetric pairs of target ions in a harmonically trapped string.

optimized pulse for Fig. 2(a) has a peak Rabi frequency of $2\pi \times 0.8 \text{ MHz}$ over $D = 20$ segments in $\tau_{\text{gate}} = 100\mu\text{s}$. The linearized pulse has a peak Rabi frequency of $2\pi \times 0.5 \text{ MHz}$ over $L = 3$ loops each with $D_{\text{loop}} = 10$ segments over a total gate time of $\tau_{\text{gate}} = 165\mu\text{s}$.

We also generate crosstalk-insensitive pulses to implement entangling gates in a 12 ion string. The gates have total duration $\tau_{\text{gate}} = 500\mu\text{s}$ split into $L = 9$ loops during each of which a component AM pulse is applied with Rabi frequencies modulated over $D_{\text{loop}} = 26$ equal-time seg-

ments. The l th loop uses a detuning $\omega_d = \nu_l - 2\pi \times 1 \text{ kHz}$, where ν_m is the frequency of the m th mode. For each neighboring or symmetric target pair, we plot in Fig. 5 the peak Rabi frequencies for the crosstalk-insensitive AM segmented gates we generate.

SI 3

The experimental demonstration of a crosstalk-insensitive two-qubit entangling gate in a three-ion string was performed using the Quantum Scientific Computing Open User Testbed (QSCOUT) at the Sandia National Laboratory [16]. On the QSCOUT platform, qubits are encoded in the hyperfine $^2S_{1/2}|F = 0, m_F = 0\rangle \equiv |0\rangle$ and $^2S_{1/2}|F = 1, m_F = 0\rangle \equiv |1\rangle$ levels of $^{171}\text{Yb}^+$ ions, with a 12.6 GHz energy splitting [43]. Raman transitions are used to apply single-qubit rotations and state-dependent forces. Our experiment used a linear chain of three $^{171}\text{Yb}^+$ ions trapped in a harmonic potential with a radial trap frequency $\omega_x = 2\pi \times 2.506 \text{ MHz}$ and axial trap frequency $\omega_z = 2\pi \times 0.7 \text{ MHz}$.

SI 4

We can derive an expression for the matrix $P^{(m)}$ in equation Eq. 6 using Eq. 4. The double time integral over τ_1 and τ_2 can be split into blocks of time during which $f(\tau_1)$ and $f(\tau_2)$ have constant peak amplitudes w_{s_1} and w_{s_2} respectively. This allows the double integral to be evaluated separately from the amplitudes encoded in the vector $w = Kx$, giving the spin-dependent phases generated in the modes the expression

$$\chi_m(\tau_{\text{gate}}) = \tilde{\chi}_m(x) := w^T P^{(m)} w = x^T K^T P^{(m)} K x \quad (12)$$

where

$$P_{s_1, s_2}^{(m)} = -\frac{1}{4} \sum_m \eta_m \begin{cases} \int_{(s_1-1)\tau_{\text{gate}}/D}^{s_1\tau_{\text{gate}}/D} \int_{(s_2-1)\tau_{\text{gate}}/D}^{\tau_1} \sin((\omega_d - \nu_k)(\tau_1 - \tau_2)) d\tau_2 d\tau_1 & \text{if } s_2 = s_1 \\ \frac{1}{2} \int_{(s_1-1)\tau_{\text{gate}}/D}^{s_1\tau_{\text{gate}}/D} \int_{(s_2-1)\tau_{\text{gate}}/D}^{s_2\tau_{\text{gate}}/D} \sin((\omega_d - \nu_k)(\tau_1 - \tau_2)) d\tau_2 d\tau_1 & \text{if } s_2 \neq s_1 \end{cases} \quad (13)$$